

Elsevier required licence: © <2018>. This manuscript version is made available under the CC-BY-NC-ND 4.0 license <http://creativecommons.org/licenses/by-nc-nd/4.0/>

31

32 **1. Introduction**

33

34 Due to rampant terrorism, governments and researchers are paying growing attention to
35 protective structures against blast and fire. UHPC is considered a desirable material for
36 this kind of structures. The Portland Cement Association (PCA) defines UHPC as "a
37 high-strength, ductile material formulated by combining portland cement, silica fume,
38 quartz flour, fine silica sand, high-range water reducer, water, and steel or organic fibers.
39 The material provides compressive strengths up to 29,000 pounds per square inch (psi)
40 and flexural strengths up to 7,000 psi". By contrast, normal strength concrete (NSC)
41 and high performance concrete (HPC) are much inferior in performance such as
42 strength, toughness, ductility and durability. In the last decades, a lot of effort has been
43 made to improve mechanical properties of UHPC. For example, most recently some
44 nano materials were investigated as a new additive to UHPCs [1, 2]. However, fire or
45 high temperature is still a great threat to all kinds of concretes including UHPCs.

46

47 Chan et al. [3] experimentally studied the behaviour of HPC subjected to high
48 temperatures up to 800 °C and they found the compressive strength of HPCs degraded
49 more sharply than NSCs. Similar findings were obtained by [4, 5]. Sobia et al. [6]
50 carried out a comparative study on ultra-high performance fibre-reinforced
51 cementitious composites (UHPRCC) before and after heat treatment. Their test
52 results revealed the residual compressive strength of UHPRCC after being exposed
53 to 1,000 °C was around 41% of its room-temperature strength. Much severer
54 deterioration was observed by [4, 7, 8]. Choe et al. [4] suggested the relative residual
55 compressive strength of ultra-high-strength concrete being heated to 1,000 °C was

56 only 2%. Another threat a fire can pose to UHPCs is explosive spalling and severe
57 explosive spillings were observed by Kahanji et al. [9, 10]. Lin et al. [11] and Akca
58 and Zihnioğlu [12] proposed that increasing pore pressure due to water evaporating and
59 thermal strain were the major reasons for concrete spalling. UHPCs usually suffer more
60 serious spalling than NSCs due to their compact structure and low porosity. Therefore,
61 it is of high significance to develop UHPCs that have better fire resistance.

62

63 Industrial by-products, such as slag and silica fume, have been widely investigated by
64 researchers as replacement of constituents of concrete to achieve environmental
65 benefit as well as better concrete performance. Steel slag is produced under a high
66 temperature of 1,650 °C so that organic, semi-volatile and volatile compounds are
67 removed. Mainly steel slag consists of calcium silicates, ferrites oxides and
68 compounds of iron, magnesium, manganese and alumina. The physical and chemical
69 analyses showed steel slag aggregate is tough, durable, and of relatively high porosity
70 and density [13]. Guo et al. [14] conducted an experimental study to investigate effect
71 of steel slag powder on workability and durability of concrete. They found compared
72 to addition of ground granulated blast furnace slag (GGBFS) alone to concrete,
73 combined admixture of GGBFS and steel slag could achieve lower dry shrinkage and
74 better abrasion resistance. Especially, when activators such as desulphurization,
75 residue sodium sulfate and desulphurization gypsum were integrated, steel slag
76 significantly improved resistance of the concrete to chloride permeation and water
77 permeation and carbonisation depth. Netinger et al. [15] studied steel slag as a coarse
78 aggregate in concrete and concluded steel slag could be an acceptable aggregate of
79 concrete for structural use and posed no risk in terms of corrosion of reinforcement.
80 Qasrawi et al. [16] investigated the effect of steel slag at different replacement ratios

81 of fine aggregate. They proposed use of steel slag in concrete could greatly enhance
82 strength of concrete, especially tensile strength, if appropriate ratio of steel slag to
83 cement was used. Effect of high temperatures on concrete with inclusion of slag has
84 also been studied by several researchers. Yüksel et al. [17] observed that the residual
85 compressive strength of specimens containing blast-furnace slag or coal bottom ash
86 was lower than the reference concrete that did not contain any slag or coal bottom ash.
87 Netinger et al. [18] suggested steel slag as coarse aggregate could improve fire
88 resistance of concrete only if it was combined with a binder that was able to better
89 adapt to slag expansion under high temperature or used as a partial replacement for
90 coarse aggregate. Silica fume is an ultra-fine reactive powder and inclusion of it can
91 improve properties of concrete particularly in compressive strength, bond strength and
92 abrasion resistance due to pozzolanic reactions between silica fume and free calcium
93 hydroxide (CH) in the cement paste [19].

94

95 To date, some efforts have been made to investigate influence of incorporation of slag
96 into UHPCs [20, 21] or other types of concretes [18, 22-24]. However, there are
97 currently very limited researches with respect to the effect of slag on the performance
98 of UHPCs subjected to high temperatures. As discussed above, UHPCs could
99 experience severe explosive spalling and suffer dramatic strength loss after being
100 exposed to elevated temperatures. On the other hand, steel slag, as a potential
101 desirable aggregate of refractory concrete, is still dumped as a land-fill material in a
102 significant amount today [13]. This study is to develop a UHPC with high fire
103 resistance. To improve fire resistance of concrete, steel fibre and polypropylene (PP)
104 fibre are usually incorporated into concrete mixtures [2, 3, 12, 25, 26]. PP fibre is
105 broadly considered beneficial to control explosive spalling since it melts at around

106 160 °C, leaving a network of escaping channels for vapour and thus helping reduce
107 internal vapour pressure [12, 27-30]. However, so far fire resistance of UHPCs
108 remains a problem of concern even though hybrid fibre is used. In the literature,
109 residual compressive strengths of UHPCs are less than 40% of their room-temperature
110 strength after being exposed to high temperatures below 1000 °C [7, 8, 25]. In this
111 study, by using steel slag as fine aggregate and incorporating other industrial
112 by-products and hybrid fibres, a UHPC with 69% relative residual strength after
113 subjected to 1000 °C has been successfully developed.

114

115 **2. Experimental details**

116

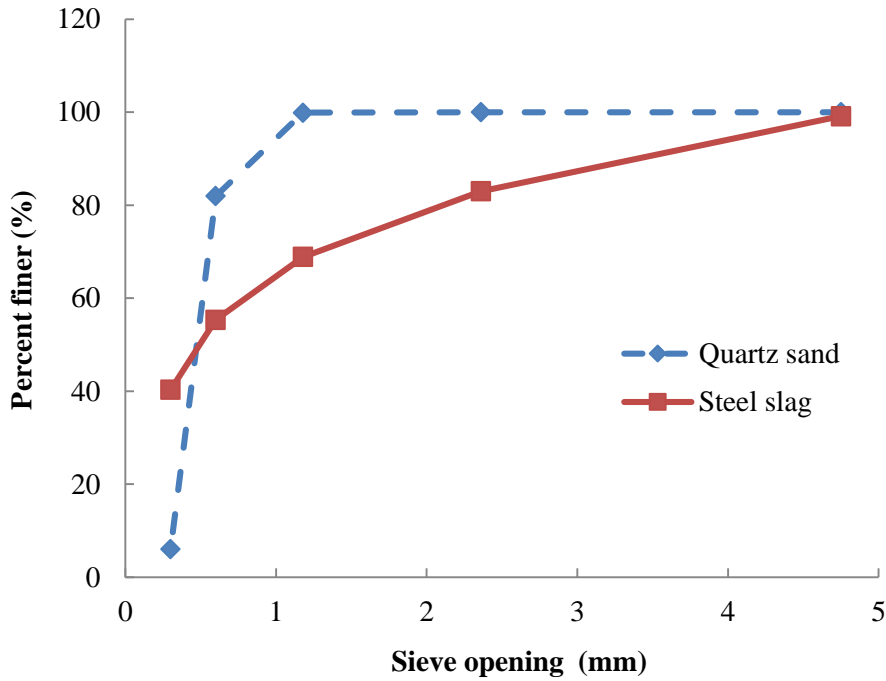
117 *2.1. Materials*

118

119 The cement used in all mixtures in this study was ordinary Portland cement (42.5
120 Grade). The silica fume added to the mixtures had a bulk weight of 200-250 kg/m³, a
121 specific surface area of 20-28 m²/g, and a particle diameter of 0.1-0.3 μm. Like
122 silica fume, fly ash is a reactive material and has pozzolanic effect in the concrete
123 mixture which helps convert free CH into calcium silicate hydrate (C-S-H) gel, so it
124 was also applied to all specimens. The fly ash had a standard spherical shape, a
125 density of 2.5×10³ kg/m³, a stacking density of 0.7×10³ kg/m³ and a thixotropic
126 index of 8. Sieve analysis was conducted on the two types of fine aggregate, i.e.
127 quartz sand and steel slag, as shown in Fig. 1. The chemical compositions of cement,
128 silica fume, fly ash and steel slag are listed in Table 1. The quartz sand has a density
129 of 2.65×10³ kg/m³, a hardness of 7 and a melting point of 1,650 °C. It needs to be
130 noted no coarse aggregate was used in any specimens, which avoided expansion

131 incompatibility between coarse aggregate and surrounding cement paste under
 132 elevated temperatures.

133



134

135 Fig. 1. Sieve analysis of quartz sand and steel slag

136

137 Table 1

138 Chemical compositions of cement, silica fume, fly ash and steel slag (%)

Materials	SiO ₂	Al ₂ O ₃	Fe ₂ O ₃	CaO	MgO	Loss of ignition
Cement	21.86	4.25	2.66	63.59	2.19	1.75
Silica fume	93.95	0.5	0.59	1.95	0.27	1.3
Fly ash	52	22	4	12	0.62	<1
Steel slag	17.03	5.64	22.69	43.38	5.98	1.56

139

140 Two types of fibre, i.e. steel fibre and PP fibre, were either or both incorporated into
 141 the UHPC mixtures (see Fig. 2). The steel fibre had a round straight shape and the

142 properties of steel fibre and PP fibre are reported in Table 2.

143



(a) Steel fibre

(b) PP fibre

144 Fig. 2. Steel fibre and PP fibre.

145

146 Table 2

147 Properties of steel fibre and PP fibre

	Length (mm)	Diameter (mm)	Density (g/cm ³)	Modulus of elasticity (GPa)	Tensile strength (MPa)	Melting point (°C)
Steel fibre	10	0.12	7.8	-	> 2500	-
PP fibre	10	0.0031	0.91	≥ 3.5	≥ 400	165

148

149 2.2. Mixture proportioning

150

151 Totally six mixtures were prepared and they were divided into two series according to
152 different fine aggregates, i.e. quartz sand or steel slag, with details shown in Table 3.

153 The series 1 used quartz sand as fine aggregate, while the series 2 used steel slag.

154 Mixtures in series 1 were divided into four categories according to fibre inclusion, i.e.
 155 no fibre, 2 vol.% steel fibre, 2 vol.% PP fibre or combination of 1 vol.% steel fibre
 156 and 2 vol.% PP fibre. Mixtures in series 2 were divided into two categories according
 157 to fibre inclusion, i.e. no fibre or combination of 1 vol.% steel fibre and 2 vol.% PP
 158 fibre. For designation of the six mixtures, the letter before the hyphen denotes the type
 159 of fine aggregates, i.e. Q for quartz sand and S for steel slag, while the letter behind the
 160 hyphen means the type of fibres, i.e. 0 for no fibre, S for steel fibre, P for PP fibre and
 161 SP for hybrid fibre. Water to binder ratio was set at 0.16 and sand to binder ratio at 1.0
 162 for all the mixtures. Unit weight for all the mixtures and slump for the mixtures Q-SP,
 163 S-0 and S-SP are listed in Table 4. The slump tests were conducted conforming to the
 164 Chinese standard GB/T 50080-2016. It can be seen the slump of the Q-SP and S-SP
 165 concretes was greatly reduced by inclusion of the hybrid fibre.

166

167 Table 3

168 Mixture proportions of UHPCs (unit: kg/m³)

Constituents	Series 1				Series 2	
	Q-0	Q-S	Q-P	Q-SP	S-0	S-SP
42.5 cement	850	850	850	850	850	850
Silica fume	137.5	137.5	137.5	137.5	137.5	137.5
Fly ash	112.5	112.5	112.5	112.5	112.5	112.5
Water	176	176	176	176	176	176
Superplasticizer	8	8	8	8	8	8
Quartz sand	1,100	1,100	1,100	1,100	-	-
Steel slag	-	-	-	-	1,100	1,100

Steel fibre	-	156	-	78	-	78
PP fibre	-	-	18.2	18.2	-	18.2

169

170 Table 4

171 Unit weight and slump of UHPC mixtures

	Q-0	Q-S	Q-P	Q-SP	S-0	S-SP
Unit weight (kg/m ³)	2,450	2,610	2,250	2,460	2,590	2,700
Slump (mm)	-	-	-	70	295	75

172

173 *2.3. Specimen preparation and tests*

174

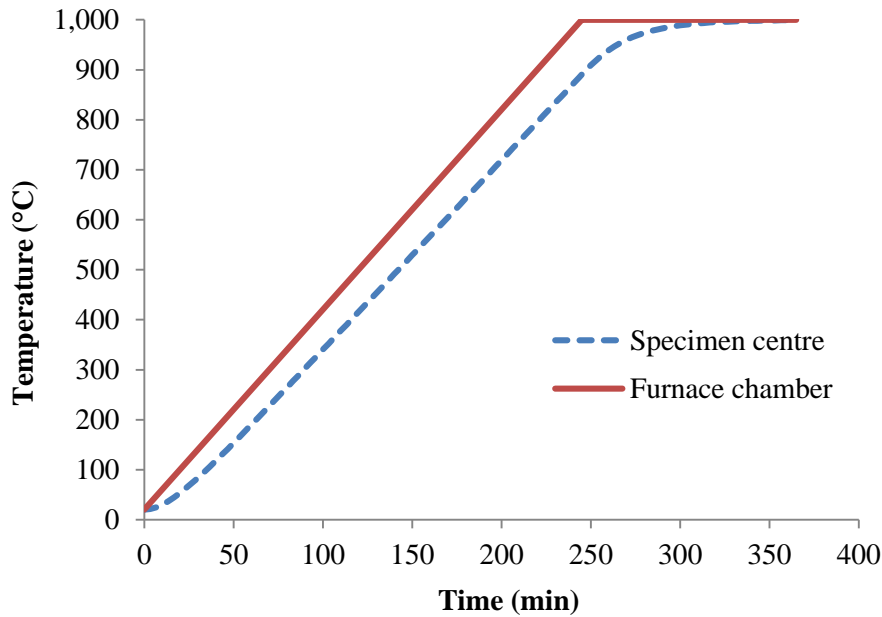
175 The compression tests were carried out for five target temperatures, i.e. 200, 400, 600,
176 800 and 1,000 °C. Under each target temperature, four specimens were prepared and
177 tested allowing for randomness of explosive spalling. There were totally 144 specimens
178 and all specimens had a cubic shape. A side length of 50 mm rather than larger was
179 chosen for all the specimens in order to avoid too frequent occurrence of explosive
180 spalling. To prepare the specimens, a forced mixer with 30 L capacity was used. Firstly,
181 the fine aggregate was fed into the mixer and mixed with a small amount of water for
182 two minutes. Then cement, silica fume and fly ash were added and mixed for five
183 minutes before water and superplasticizer were poured. The mixing process continued
184 for another eight minutes. Finally, fibres were added to the mixture and mixed for five
185 more minutes before the mixture was cast in the steel moulds. 24 hours later, the
186 specimens were demoulded and put into a water tank with thermostatic control, where
187 they were submerged by hot water of constant 90 °C for one day in order to accelerate

188 pozzolanic reaction. Then, they were cured under a standard curing condition for 28
189 days. Before heating, a drying treatment is usually needed to control explosive
190 spalling. Okpala [31] used a mechanically ventilated oven to dry the paste and mortar
191 specimens at 105 ± 1 °C for a duration of 5-6 days. However, after a comparative
192 study of different drying temperatures and facilities, Gallé [32] suggested 105 °C could
193 be too high to prevent microstructure of the specimen from being impacted by oven
194 drying treatment. In this study, the specimens were put into an electric furnace for a
195 drying treatment under a temperature of 90 °C for 24 hours, which proved to be an
196 effective means to control explosive spalling. Since all the six UHPC mixtures were
197 prepared with the identical water content, i.e. 176 kg/m^3 , and experienced the same
198 procedure of curing and drying, it was supposed they had the similar initial moisture
199 level.

200

201 The specimens were heated in an electric furnace with a heating capability of 1400 °C.
202 Real fire condition could be simulated as per the heating curve defined in the standards
203 ISO 834 [33] which has an exponential relationship between growing temperature and
204 heating time. However, to make the heating process simple, some researchers such as
205 [34] applied a constant heating rate of 5 °C/min according to the standards ASTM E831
206 [35]. In this study, 4 °C/min was selected as the heating rate according to ASTM E831
207 [35] and 1 and 8 °C/min heating rates were chosen to make a comparison study in
208 subsection 3.2.1. Compact concrete like UHPC is vulnerable to explosive spalling
209 when being heated. To prevent damage to the furnace and ensure safety, silicon boards
210 were mounted on the chamber inner walls of the furnace. Furthermore, a steel cage
211 was presented inside the furnace to contain specimens being heated. At a time, four
212 specimens were heated at a rate of 4 °C/min until reaching the target temperatures and

213 then they remained subjected to the constant target temperatures for another period of
214 time or called holding time to achieve uniformly distributed temperatures throughout
215 the specimen. The holding time, according to Chen et al. [36], has a significant impact
216 on stress-strain behaviour of concretes exposed to high temperatures. To determine an
217 appropriate holding time, a heating simulation with target temperature 1000 °C was
218 conducted using the thermal parameters from the European standard [37]. Fig. 3
219 shows the temperature time-history in the furnace chamber and at the centre of the
220 model. It can be seen after 2 hours holding time (from 245 to 365 min), the
221 temperature at the specimen centre is 999.3 °C, very close to the target temperature.
222 For target temperatures lower than 1000 °C, the temperature gap between the furnace
223 chamber and the centre of the model is smaller, as shown in Fig. 3. Because concrete
224 has higher thermal conductivity and lower specific heat under lower temperatures, it is
225 no doubt the valid holding time for higher target temperature ensures uniform
226 temperature distribution in case of lower target temperatures. Hence, in this study the
227 holding time for all specimens was consistently set at 2 hours to ensure uniformly
228 distributed temperatures, at the same time to avoid impact of this factor. Afterwards,
229 the furnace door was opened to let the specimens cool down to room temperature. It
230 should be noted in this study temperatures were measured by the thermocouple
231 mounted on the internal wall of the furnace unless specified otherwise.
232



233

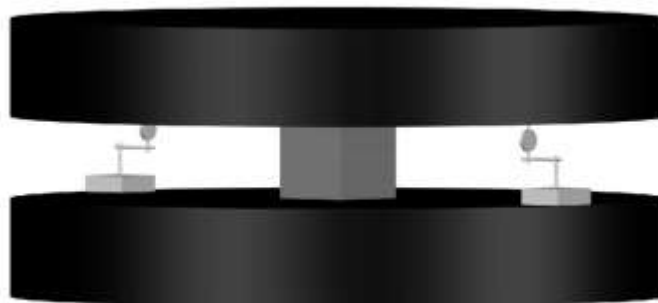
234 Fig. 3. Comparison of temperature time-history between furnace chamber and
 235 specimen centre under target temperature 1000 °C

236

237 Compressive tests were implemented on a 1,000 kN capacity electrohydraulic servo
 238 pressure testing machine, with the procedure conforming to the Chinese standard
 239 JGJ70-2009. The loading rate was controlled at 0.2 mm/min and the loading and
 240 displacement data were recorded automatically. To measure the displacement, two
 241 displacement gauges were symmetrically mounted on the two sides of the specimen
 242 between the loading plates, as illustrated in Fig. 4. In this study, the compressive
 243 strength was calculated as the average value of four specimens. Results for all mixtures
 244 are reported in Table 5, where f_c denotes compressive strength of the specimens which
 245 were not exposed to high temperatures (i.e. control specimens), f_{cT} denotes
 246 compressive strength of the specimens which were exposed to high temperatures and
 247 f_{cT} / f_c means normalised compressive strength. It should be noted while most of the test
 248 results were an average of four specimens, some came from three due to explosive
 249 spalling. Due to severe explosion, data for the mixtures Q-0, Q-S and S-0 were not

250 recorded above 200 °C.

251



252

253

Fig. 4. Sketch of testing setup.

254

255 Table 5

256 Compressive strength under various temperatures

Tempera- ture (°C)		Q-0	Q-S	Q-P	Q-SP	S-0	S-SP
20	f_c (MPa)	112.4	187.5	125.5	162.1	90.0	162.8
200	f_{cT} (MPa)	164.7	204.8	132.5	176.2	191.0	182.5
	f_{cT}/f_c	1.47	1.09	1.06	1.09	2.12	1.12
400	f_{cT} (MPa)	-	-	163.5	230.1	-	215.9
	f_{cT}/f_c	-	-	1.30	1.42	-	1.33
600	f_{cT} (MPa)	-	-	112.3	153.8	-	208.3
	f_{cT}/f_c	-	-	0.89	0.95	-	1.28
800	f_{cT} (MPa)	-	-	38.1	40.0	-	147.6
	f_{cT}/f_c	-	-	0.30	0.25	-	0.91
1,000	f_{cT} (MPa)	-	-	37.5	40.4	-	112.8

$$f_{cT}/f_c \quad - \quad - \quad 0.30 \quad 0.25 \quad - \quad 0.69$$

257

258 **3. Results and discussion**

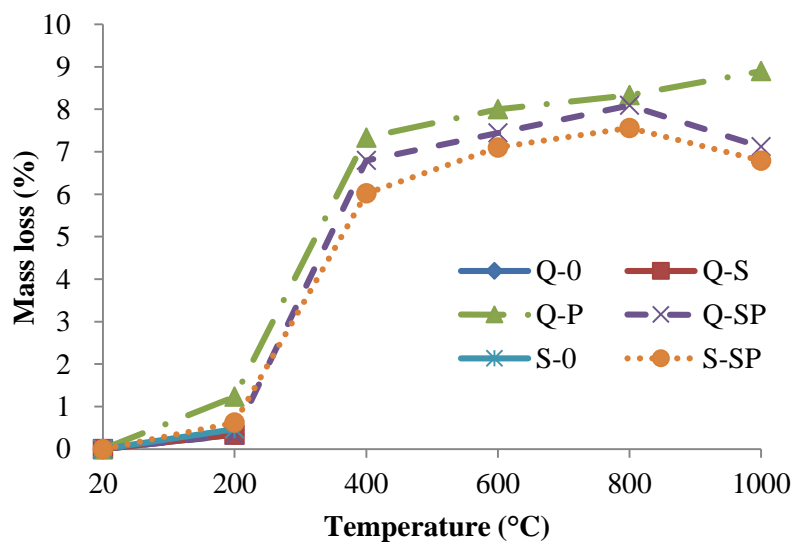
259

260 *3.1. Mass loss*

261

262 In this paper, mass loss refers to water evaporation and gas escape from UHPCs being
 263 heated. The relationship between mass loss and temperature for all the mixtures is
 264 depicted in Fig. 5. It can be seen all mixtures had a small mass loss below 200 °C,
 265 indicating the UHPC specimens had a very compact structure which hindered vapour
 266 from escaping. For mixtures without PP fibres, i.e. the Q-0, Q-S and S-0 concretes, data
 267 were not recorded above 200 °C due to the severe explosion. Being heated to 200 °C,
 268 both the Q-0 and the Q-S specimens experienced an average mass loss of 1 g or 0.34%
 269 in percentage, indicating steel fibre had little influence in mass loss of UHPCs
 270 exposed to elevated temperatures below 200 °C. The mass loss of the other three
 271 mixtures containing PP fibres increased sharply between 200 °C and 400 °C. It was
 272 because the PP fibres melting at 165 °C provided a network of escaping channels for
 273 the vapour, while a majority of vapour came from the capillary water and bound water
 274 between 200 °C and 400 °C. Research conducted by Tsuchiya and Sumi [38] revealed
 275 between temperature range of 360 to 400 °C PP could decompose into various
 276 volatiles such as Pentane and Propylene, which was another contribution of the mass
 277 loss. Then with temperature growing from 400 °C to 1,000 °C, the mass loss rose
 278 slightly and peaked at around 8%. It can be seen from Fig. 5 that the mass loss of the
 279 Q-P mixture was a little higher than the Q-SP and the S-SP mixtures. The reason
 280 could be the Q-P concrete didn't contain steel fibres and thus suffered severer cracking

281 and spalling, which boosted the escaping of vapour and smoke. Another possible
 282 reason could be the Q-P concrete as an exception might have more moisture or higher
 283 pore volume. The S-SP concrete suffered the smallest mass loss among the three
 284 mixtures containing PP fibres, indicating this mixture had more compact structure
 285 than the Q-SP concrete, which agreed with the fact that the latter had a lower
 286 probability of occurrence of explosive spalling than the former. From 800 °C to
 287 1,000 °C, the mass loss of Q-SP and S-SP concretes decreased because they took in
 288 moisture from the air during a one-day cooling.
 289



290

291 Fig. 5. Mass loss under different temperatures.

292

293 3.2. Explosive spalling

294

295 3.2.1. Effect of heating rate on explosive spalling of the Q-S concrete

296

297 To investigate the effect of heating rate on explosive spalling of heated UHPCs, three
 298 heating rates, i.e. 1, 4 and 8 °C/min, were applied to the Q-S concrete. The target

299 temperature under 1 and 4 °C/min heating rates was set at 400 °C, while under
300 8 °C/min was set at 600 °C.

301

302 The spalling details of the Q-S concrete are reported in Table 6. It was observed under
303 whatever heating rates all the specimens suffered serious explosive spalling, which
304 suggested the heating rate had nothing to do with the probability of explosive spalling
305 in the case of Q-S concrete that was very dense and without PP fibres. However, with
306 the increase of heating rate, the explosive spalling started and ended earlier, both the
307 spalling starting temperature and the spalling ending temperature became higher, and
308 the smoke escaping temperature range became on a higher level. During the heating,
309 there were several intense explosions happening under whatever heating rates, with big
310 burst sounds being heard. Each intense explosion came with the escape of a large
311 amount of vapour and dust, which could be observed outside the furnace. This
312 phenomenon indicated that the accumulation of internal vapour pressure was a big
313 contribution of the explosive spalling.

314

315 Table 6

316 Details of explosive spalling of Q-S concrete at different heating rates

Heating rate (°C/min)	1	4	8
Target temperature (°C)	400	400	600
Probability (%)	100	100	100
Starting time (min) ^a	325	92	35
Ending time (min) ^a	460	113	67
Starting temperature (°C) ^b	323	357	422
Ending temperature (°C) ^b	400	400	563

Smoke escaping temperature range (°C)^c 350-391 369-400 460-553

317 ^a Starting time is the time when spalling was first observed, while ending time is the
318 time after which spalling would no longer occur.

319 ^b Starting temperature is the temperature at which spalling was first observed, while
320 ending temperature is the temperature above which spalling would no longer occur.

321 ^c Smoke escaping temperature is the temperature range only within which smoke was
322 observed.

323

324 Table 7 shows the explosive spalling of the Q-S specimens heated under the three
325 heating rates. It can be seen with higher heating rate and higher target temperature the
326 debris of the specimens tended to be smaller, indicating more intense explosive
327 spalling.

328

329 Table 7

330 Explosive spalling of Q-S concrete at different heating rates

Heating rate
(°C/min)

1





331

332 *3.2.2. Explosive spalling of specimens without PP fibres*

333

334 In this subsection, the explosive spalling of the mixtures without PP fibres, i.e. Q-0, Q-S
 335 and S-0, were compared under the identical target temperature of 400 °C and heating
 336 rate of 4 °C/min. The details of the explosive spalling are listed in Table 8 and Table 9
 337 and the sieving results of debris are shown in Fig. 6. All the mixtures suffered explosive
 338 spalling when being heated to the target temperature as shown in Table 8 and broke into
 339 pieces as shown in Table 9. Accompanying each explosive spalling, it was observed
 340 that some vapour was intensively released. This phenomenon indicated the built-up
 341 vapour pressure was an important contribution to the explosive spalling.

342

343 Compared with the Q-0 concrete without any fibres, the Q-S concrete reinforced with 2
 344 vol.% steel fibres started exploding at a higher temperature. It was because explosive
 345 spalling would not happen until the internal vapour pressure was greater than the tensile
 346 strength of the concrete which was considerably increased by the addition of steel fibre.
 347 The S-0 concrete which had steel slag as fine aggregate had almost the same spalling

348 starting time but higher starting temperature in comparison with the Q-0 and Q-S
 349 concretes which had quartz sand as fine aggregate.

350

351 Table 8

352 Details of explosive spalling of mixtures without PP fibres at heating rate of 4 °C/min

Mixture	Q-0	Q-S	S-0
Target temperature (°C)	400	400	400
Probability (%)	100	100	100
Starting time (min) ^a	86	92	92
Ending time (min) ^a	109	113	147
Starting temperature (°C) ^b	338	357	385
Ending temperature (°C) ^b	400	400	400

353 ^{a,b} Same as in Table 6.

354

355 Table 9

356 Explosive spalling of mixtures without PP fibres at heating rate of 4 °C/min

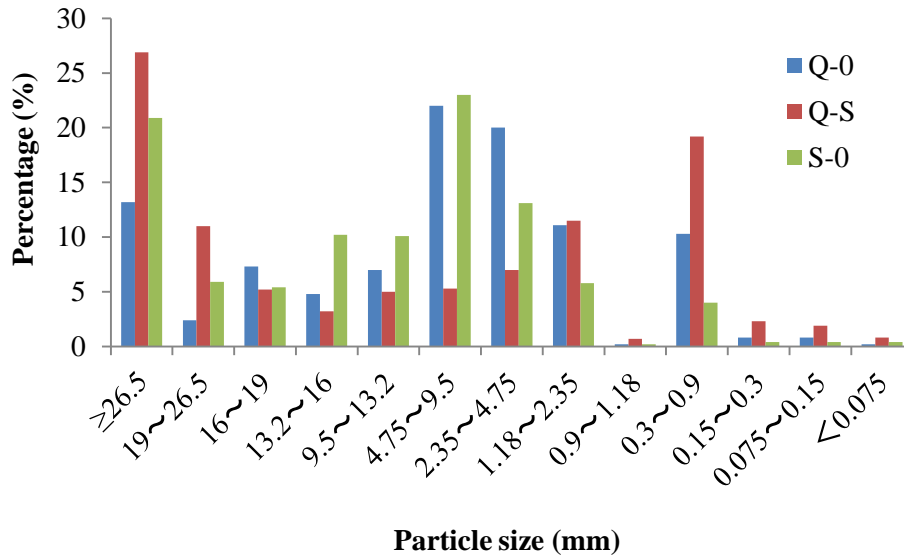
Mixture			
Q-0			



357

358 Fig. 6 exhibits sieving results of debris of the three mixtures without PP fibres, which
359 reflects effect of steel fibre and difference between the two types of aggregate on
360 explosive spalling. Among the three mixtures, the Q-S concrete had the greatest
361 proportion in both large and small debris sizes as shown in Fig. 6. The steel fibres
362 bridged the gaps when the cracks were growing and thus restrained propagation of the
363 cracks, which helped the Q-S concrete remain more large-size debris than the other two
364 without steel fibres. On the other hand, the constraint effect of the steel fibres caused
365 greater vapour pressure, which resulted in more small-size debris after the specimens
366 exploded. Compared to the Q-0 concrete, the S-0 concrete containing steel slag had a
367 higher percentage of debris with sizes over 4.5 mm. The reason could be the steel slag
368 produced under 1,650 °C had relatively high thermal stability and similar chemical
369 compositions to the cement, which reduced thermal incompatibility between the fine
370 aggregate and the cement paste.

371



372

373 Fig. 6. Sieving results of debris of mixtures without PP fibres.

374

375 *3.2.3. Explosive spalling of specimens with PP fibres*

376

377 As discussed above, PP fibre, which melts at about 165 °C, helps release vapour
 378 pressure and thus reduces the risk of explosive spalling when concrete is exposed to
 379 elevated temperatures. In this subsection, three mixtures containing PP fibres, i.e., the
 380 Q-P, Q-SP and S-SP concretes, are compared in terms of explosive spalling. The three
 381 concretes were heated to five target temperatures, i.e. 200, 400, 600, 800 and 1,000 °C,
 382 with explosive spalling details reported in Table 10. Spalling damage of these
 383 specimens is displayed in Table 11, where unheated specimens are also listed in order to
 384 make a comparison.

385

386 Table 10

387 Details of explosive spalling of mixtures with PP fibres under different target
 388 temperatures

Target temperature (°C)	Spalling probability (%)			Spalling temperature range (°C)		
	Q-P	Q-SP	S-SP	Q-P	Q-SP	S-SP
200	0	0	0	-	-	-
400	0	0	50	-	-	392-400 ^a
600	75	50	50	404-458	447-464 ^a	467-503 ^a
800	75	0	50	409-472	-	391-440 ^a
1,000	100	50	25	413-463	437-457 ^a	464 ^a

389 ^a Only slight spalling was observed.



















390

391 From Table 10 and Table 11, it can be seen all the specimens didn't experience
392 explosive spalling at the target temperature of 200 °C. Under the 400 °C target
393 temperature, half of the four S-SP specimens suffered slight spalling but the other two
394 remained intact. With target temperature over 600 °C, all the specimens experienced
395 spalling to some degree, which occurred between 391 °C and 503 °C. However, unlike
396 in the tests of the mixtures without PP fibres, no intensive release of vapour was
397 observed coming with any of the spalling. The spalling could result from thermal stress
398 and incompatibility between the aggregate and the cement paste but not vapour
399 pressure. It can also be seen from Table 10 and Table 11 that the Q-P concrete which
400 had only PP fibres suffered more frequent and severer spalling than the other two
401 reinforced with hybrid fibres. Steel fibre failed to prevent the occurrence of explosion
402 resulting from built-up vapour pressure as discussed in subsection 3.2.2, but it reduced
403 probability and intensity of spalling resulting from thermal stress and incompatibility
404 between the aggregate and the cement paste. When being heated from 20 °C to 1,000 °C,
405 all the specimens experienced a colour change from grey to grey-white and then amber,
406 as shown in Table 11.

407

408 Table 11

409 Explosive spalling of mixtures with PP fibres under different temperatures

Tempera- ture (°C)	Q-P	Q-SP	S-SP
20			
200			
400			
600			
800			
1,000			

410

411 3.3. Compressive tests

412

413 3.3.1. Specimens without PP fibres

414







415 Because of severe explosive spalling when being heated to 400 °C and above, the
416 specimens without PP fibres were tested only at room temperature and 200 °C. For the
417 compressive tests, failure forms of the three mixtures, i.e. Q-0, Q-S and S-0, are

418 displayed in Table 12. Without addition of any fibres, both the Q-0 and S-0 concretes
 419 suffered brittle damage and were crushed up under either temperature. By contrast,
 420 the Q-S concrete reinforced with steel fibres improved a lot in ductility and remained
 421 its integrity under the compressive loading. The UHPC mixtures had highly compact
 422 structure, leading to reduced relative stiffness to the steel loading plate. The internal
 423 energy of the loading plate building up during the loading procedure was released
 424 suddenly when the specimen yielded, which resulted in the crush of the specimens
 425 without steel fibres due to inadequate tensile strength.

426

427 Table 12

428 Failure forms of mixtures with PP fibres under different temperatures

Tempera- ture (°C)	Q-0	Q-S	S-0
20			
200			

429

430 Stress-strain curves for the three mixtures under room temperature and 200 °C are
 431 shown in Fig. 7. It can be seen that at 200 °C all the three mixtures enjoyed an
 432 improvement of compressive strength in comparison with at room temperature. The
 433 reason could be that high-pressure moisture failing to escape due to the tight structure
 434 of the UHPC specimen created an enclosed high-temperature and high-pressure curing
 435 environment or "internal autoclaving" [39]. This curing environment greatly boosted

436 both cement hydration and pozzolanic reactions due to the presence of active SiO_2 ,
437 from silica fume and fly ash, generating more C-S-H gel. There the C-S-H gel was
438 transformed into xonotlite and tobermorite, which made the internal structure of the
439 specimen even more compact and thus enhanced its compressive strength. As shown
440 in Table 5, when being heated to 200 °C the Q-0 concrete had a 47% increase of
441 compressive strength, while it was only 6% for the Q-P concrete in comparison with
442 their respective original room-temperature strength. It was because PP fibre enhanced
443 the room-temperature strength of the Q-P concrete but its melting at 165 °C made this
444 enhancement invalid. On the other hand, the melting of PP fibres left pores in the
445 concrete, which resulted in more cracks when the concrete was under pressure and
446 reduced moisture pressure due to the release of vapour. These weakened the boost
447 effect resulting from the high-temperature and high-pressure curing environment. From
448 Table 5, it can also be seen the Q-S concrete had an unimpressive 9% improvement of
449 compressive strength compared to 47% for the Q-0 concrete and 112% for the S-0
450 concrete when exposed to 200 °C. The reason is the Q-S concrete reinforced with steel
451 fibres had comparatively high compressive strength at room temperature. Fig. 7 also
452 shows the Q-S concrete had much higher ductility and toughness than the other
453 concretes under either temperature.

454

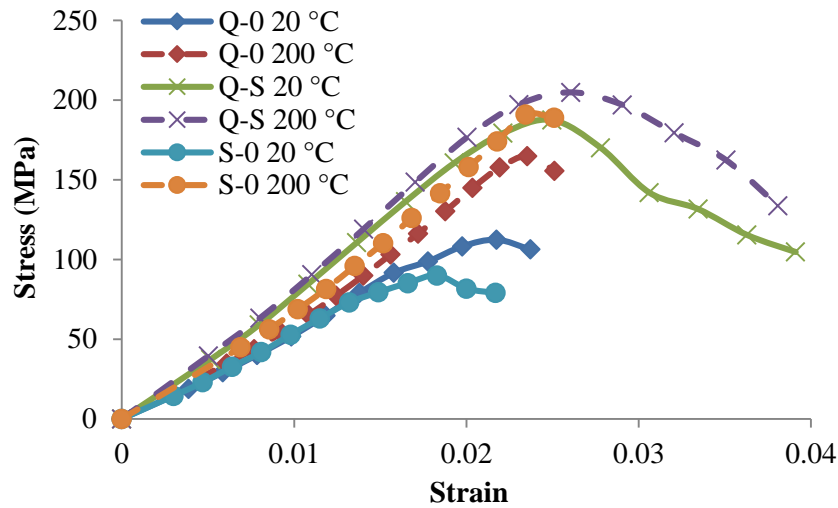


Fig. 7. Stress versus strain curves.

455

456

457

458 3.3.2. Specimens with PP fibres

459
















460 Table 13 shows the failure forms of the three mixtures containing PP fibres exposed to
 461 temperatures ranging from 20 °C to 1,000 °C. As can be seen, the Q-P concrete
 462 suffered a ductile damage at room temperature, but under temperatures 200, 400 and
 463 600 °C its damage was in a brittle manner. It was because the PP fibres improved the
 464 ductility of the Q-P concrete under room temperature. However, when it was heated to
 465 200 °C and above, the melted PP fibres resulted in deterioration of ductility of the
 466 concrete. Under 800 °C and 1,000 °C, the Q-P concrete exhibited a ductile failure mode
 467 again. This was because the concrete had been loosened and softened. Rashad et al. [39]
 468 pointed out coarsening of pore-structure can happen when cement paste is heated to
 469 400 °C and above and C-S-H can be dramatically decomposed at 600 °C and above,
 470 which may lead to concrete loosening and softening and cohesiveness deterioration of
 471 cement paste. Due to the cohesiveness deterioration of the cement paste, a double
 472 pyramid was formed during the compressive test on the Q-P concrete subjected to
 473 800 °C and 1,000 °C, as shown in Table 13. Compared to the Q-P concrete, the Q-SP

474 and S-SP concretes experienced ductile damage forms under compression throughout
 475 all the target temperatures from 20 °C to 1,000 °C. Not only did the addition of hybrid
 476 fibres restrain occurrence of severe explosive spalling, but also it greatly improved the
 477 ductility of the concrete exposed to high temperatures. Under 1,000 °C, however, the
 478 Q-SP and S-SP concretes had the similar failure form to the Q-P concrete. This could be
 479 attributed to the loss of strength of steel fibres under high temperatures. According to
 480 the European standard [40], under 800 °C and 1,000 °C steel retains only 11% and 4%
 481 of its yield strength respectively.

482

483 Table 13

484 Compressive failure forms of mixtures with PP fibres under different temperatures

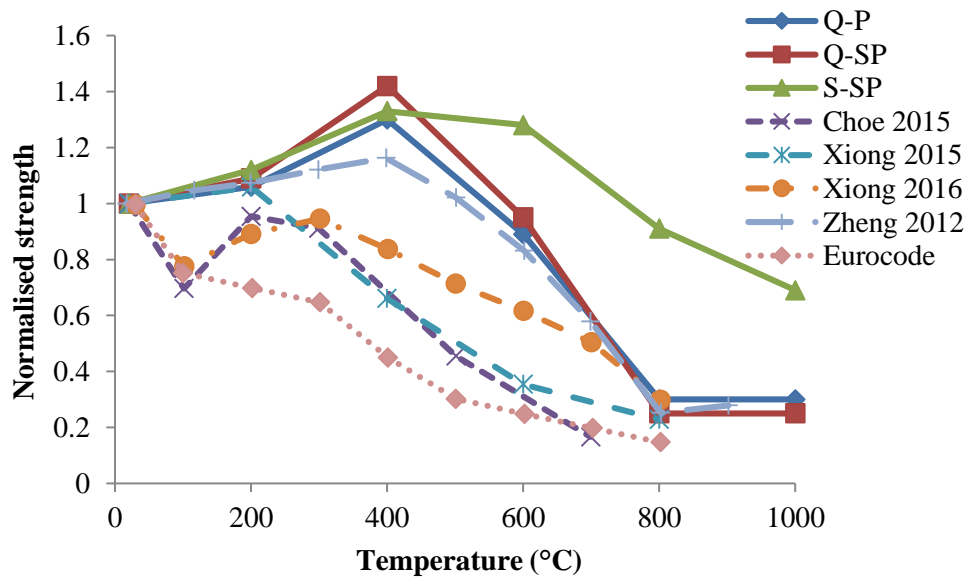
Tempera- ture (°C)	Q-P	Q-SP	S-SP
20			
200			
400			
600			
800			



485

486 The relationships between compressive strength and temperature for the three
 487 concretes are illustrated in Fig. 8. With the target temperature ascending from 20 °C to
 488 400 °C, all the three concretes made an improvement in compressive strength. From
 489 room temperature to 200 °C, the enhancement mechanism is the same as discussed in
 490 subsection 3.3.1. From 200 °C to 400 °C, more C-S-H gel was produced and
 491 transformed into xonotlite and tobermorite as pozzolanic reactions continued under
 492 the high-temperature and high-pressure environment. In addition, evaporation of
 493 bound water made the cement paste more compact and harder. Also during this stage,
 494 PP fibres melted completely, greatly relieving vapour pressure. All these contributed
 495 to an enhancement of compressive strength of the three concretes.

496



497

498 Fig. 8. Normalised compressive strength versus temperature.

499

500 In contrast, from 400 °C to 800 °C all the three concretes suffered a strength decrease. It

501 can be seen from Fig. 8, the strength loss of the Q-SP concrete was a little steeper than
502 that of the Q-P concrete, while the S-SP concrete had a much slower deterioration of
503 strength than the other two. During this stage, decomposition of the CH occurred
504 between approximately 430 °C and 600 °C, while for the C-S-H it started at around
505 560 °C and then became significant above 600 °C [39]. A large amount of C-S-H was
506 transformed into C_3S and $\beta-C_2S$ and $\alpha-SiO_2$ was transformed into $\beta-SiO_2$, which
507 resulted in increased porosity in the paste [41]. At 800 °C, the C-S-H was completely
508 decomposed and the $CaCO_3$ started to decompose, contributing to decreased
509 compactness of the internal structure and a lot of small cracks on the surfaces of the
510 specimen. Also, at this stage, the mismatching volume expansion between the cement
511 paste and the aggregate played a significant role that worsened the mechanical
512 performance of the concrete [13, 18].

513

514 From 800 °C to 1,000 °C, the strength of the Q-P and Q-SP concretes remained almost
515 the same but that of the S-SP concrete kept falling. However, the S-SP concrete
516 retained a relatively high residual strength of 112.8 MPa or normalised residual
517 strength of 69% after being exposed to 1,000 °C, while that for the Q-P and Q-SP
518 concretes was only 40 MPa or below 30%.

519

520 Fig. 8 also shows the results of UHPCs from other researches [4, 7, 8, 25] and high
521 strength concrete according to the European standard EN 1992-1-2 [37]. It can be
522 seen over 600 °C the S-SP concrete retained markedly higher normalised strength than
523 the other concretes. The main reason could be, on one hand, adding steel slag to the
524 mixture reduced the amount of CH formed during the hydration, which increased the
525 fire resistance of the mixture exposed to elevated temperatures [42, 43]. On the other

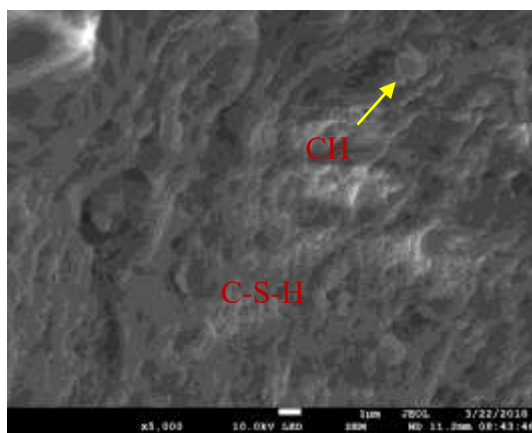
526 hand, steel slag usually has rough surfaces and thus improves properties of interfacial
527 transition zone (ITZ), which could be critical for concrete under high temperatures.
528 Research conducted by Jia [44] revealed NSC exposed to high temperatures above
529 300 °C exhibited different damage modes under compressive loading. The damage
530 occurred along the ITZ or within the paste other than running through the aggregate
531 which was the case for unheated concretes, indicating high temperature could severely
532 degrade properties of ITZ. Ducman and Mladenović [13] and Netinger et al. [18]
533 suggested a major factor contributing to strength loss of concrete using steel slag as
534 aggregate is the expansion of steel slag in contrast to the shrinkage of cement paste after
535 exposed to high temperatures. However, in this study steel slag was used as fine
536 aggregate and most of it had a size smaller than 2.5 mm, which could mitigate the
537 negative effect of volume mismatching between the steel slag and the cement paste.
538 Besides, as discussed in subsection 3.2, steel slag had excellent thermal stability and
539 similar chemical compositions to cement, which reduced thermal incompatibility
540 between the fine aggregate and the cement paste and could improve residual
541 properties. From Fig. 8, it can also be seen the S-SP concrete was the only one that had
542 its strength under 600 °C higher than its room-temperature strength.

543

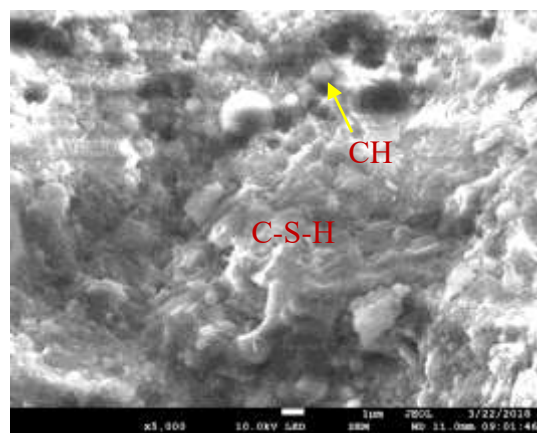
544 Fig. 9 shows the SEM analysis of the S-SP concrete after exposure to temperatures from
545 20 °C to 800 °C, using a JEOL JSM-7800F SEM. For the S-SP specimen never
546 subjected to an elevated temperature, it had continuous and compact C-S-H phase and
547 scattered CH crystals. After exposed to 200 °C, the C-S-H phase in the concrete
548 remained continuous and became more compact while the CH crystals became fewer
549 and smaller. However, due to melting of PP fibre and cracking resulting from vapour
550 pressure, the matrix presented a rougher surface. After subjected to 400 °C, the C-S-H

551 phase had even more compact structure and better integrity while the CH phase
552 continued to reduce in quantity and size. Suffering 600 °C, the C-S-H phase lost some
553 continuity and integrity due to decomposition and became less compact. At the same
554 time, the CH phase completely decomposed. At 800 °C, the C-S-H phase did not exist
555 any longer and the matrix was honeycombed, resulting in greatly worsened concrete
556 performance.

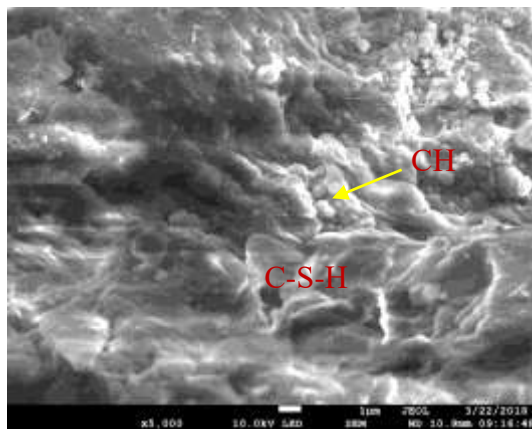
557



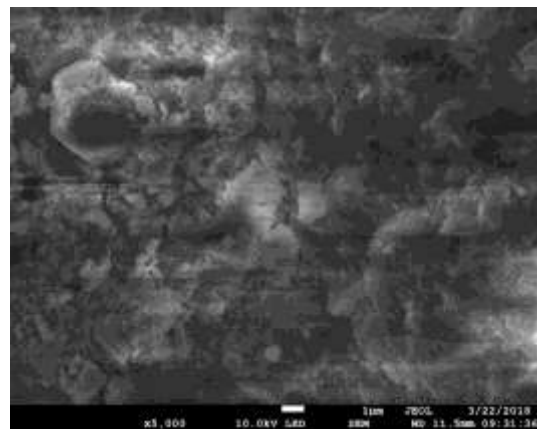
(a) 20 °C



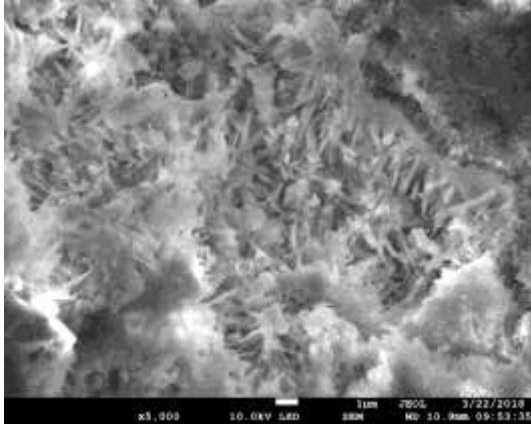
(b) 200 °C



(c) 400 °C



(d) 600 °C



(e) 800 °C

558 Fig. 9. SEM analysis of S-SP concrete after exposure to different temperatures.

559

560 The stress-strain curves of the three concretes under different temperatures from 20 °C

561 to 1,000 °C are depicted in Fig. 10, Fig. 11 and Fig. 12, respectively. It can be seen the

562 stress-strain curves of the Q-P and the Q-SP concretes had the similar varying pattern

563 under different temperatures. For example, both the concretes suffered a significant

564 drop in strength and modulus elasticity when being heated to 600 °C and above and had

565 a flattened stress-strain curve under 800 °C and 1,000 °C. As discussed above, the

566 concretes were loosened and softened when being heated to higher than 800 °C.

567 Nevertheless, due to the addition of steel fibres, the Q-SP concrete exhibited greater

568 ductility and toughness than the Q-P concrete under whatever temperatures. From Fig.

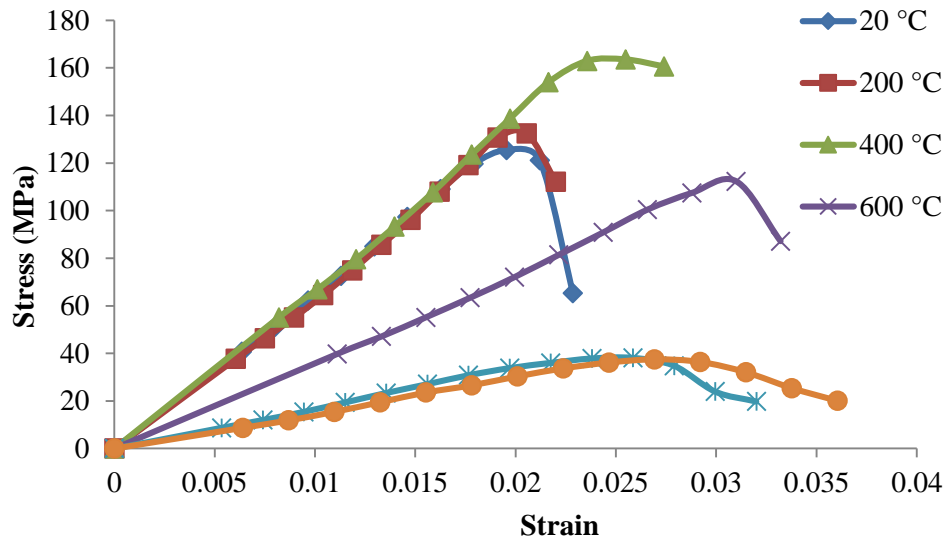
569 12 it can be seen even under 600 °C the S-SP concrete had strength much higher than its

570 room-temperature strength and relatively high modulus elasticity. Under higher

571 temperatures up to 1,000 °C, the S-SP concrete retained relatively high residual

572 strength and modulus elasticity in comparison with the Q-P and the Q-SP concretes.

573

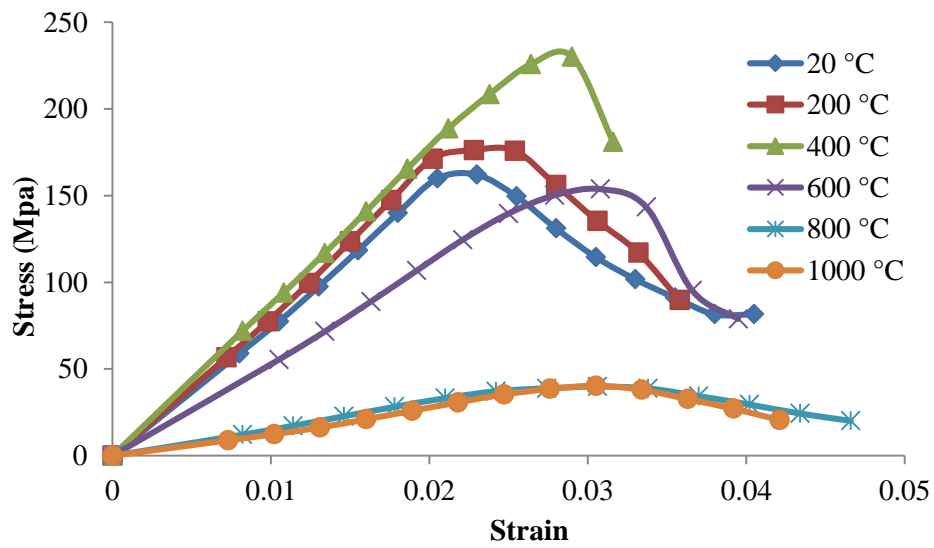


574

575

Fig. 10. Stress versus strain curves of Q-P concrete.

576

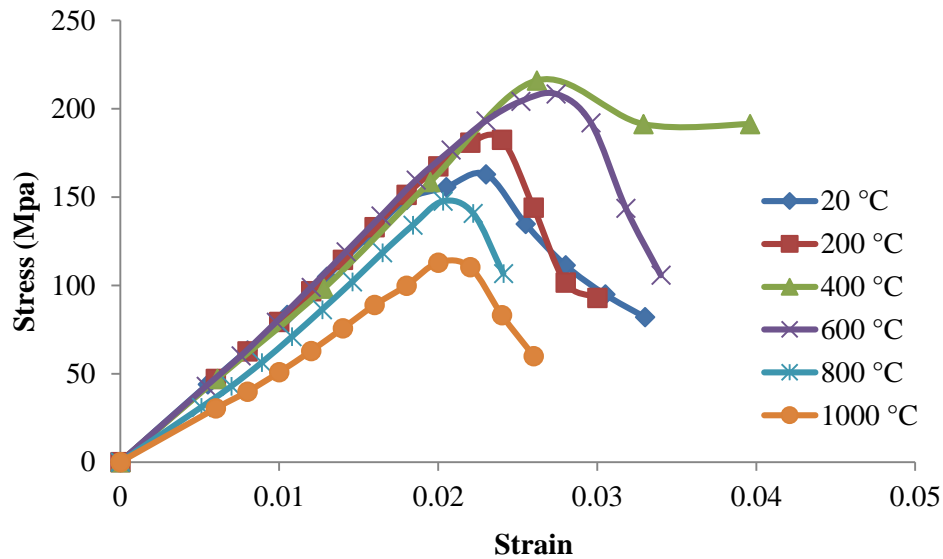


577

578

Fig. 11. Stress versus strain curves of Q-SP concrete.

579



580

581

Fig. 12. Stress versus strain curves of S-SP concrete.

582

583

584

585

586

587

588

589

590

591

592

593

Fig. 13 shows relationships between normalised modulus of elasticity and temperature of the three UHPC mixtures as well as light weight concrete from the European standard EN 1992-1-2 [37]. It should be noted modulus of elasticity here was calculated as the slope between two points on the ascending portion of stress-strain curves corresponding to 60% and 40% of peak stress respectively, which was also adopted by Su et al. [45]. The curves for the three UHPCs in Fig. 13 has a similar pattern to those in Fig. 8, though increase of modulus of elasticity was much less impressive than that of strength from 20 °C to 600 °C. It can also be seen the degradation of modulus of elasticity of concrete specified in the European standard EN 1992-1-2 [37] is much severer than the three UHPCs under whatever elevated temperatures.

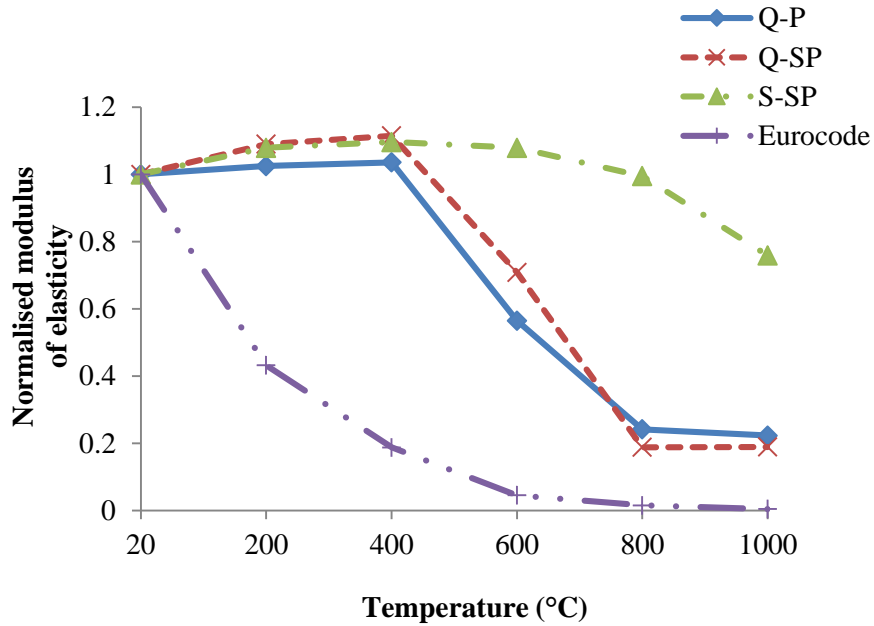


Fig. 13. Normalised modulus of elasticity versus temperature.

4. Conclusions

To develop a UHPC with excellent fire resistance, a total of six UHPC mixtures were designed using quartz sand or steel slag as fine aggregate, with or without steel fibre, PP fibre or hybrid fibre. Special attention was paid to explosive spalling of UHPCs subjected to elevated temperatures since UHPCs are usually of compact structure and thus vulnerable to explosive spalling. Besides, residual compressive strengths and stress-strain relationships of the UHPC mixtures are discussed after they were heated to elevated temperatures up to 1,000 °C. The following conclusions could be drawn from the test results and the above analysis:

1. Most mass loss of the mixtures with PP fibre happened between 200 °C and 400 °C due to water evaporation and PP volatilisation.
2. Heating rate had little effect on explosive spalling occurrence of the Q-S mixture, which had very dense matrix without PP fibres. However, higher heating rate could

611 result in more intense explosive spalling.

612 3. Vapour pressure was a significant contribution to explosive spalling. PP fibre was an
613 effective additive to control explosive spalling, though failed to eliminate it
614 completely. Steel fibre could reduce the probability and intensity of spalling
615 resulting from thermal stress and incompatibility between aggregate and cement
616 paste.

617 4. A UHPC mixture with excellent fire-resistance properties was successfully
618 developed. After being exposed to 1,000 °C, it retained 69% of its original
619 compressive strength, much higher than the existing concretes. Reinforced with
620 hybrid fibre, this concrete also greatly decreased the occurrence of explosive
621 spalling.

622 5. Addition of steel slag to UHPC mixtures reduced amount of CH formed during
623 hydration. With rough surface, steel slag could improve ITZ properties of UHPCs
624 exposed to elevated temperatures. Having high thermal stability and similar
625 chemical compositions to cement, steel slag as fine aggregate also relieved thermal
626 incompatibility between aggregate and cement paste. These features of steel slag
627 may significantly improve residual properties of UHPCs using steel slag as fine
628 aggregate.

629

630 **Acknowledgement**

631

632 The authors gratefully acknowledge the financial support of the Australian Research
633 Council grant DP160104661, the National Basic Research Programme 2015CB058002
634 and the Australian Government Research Training Program Scholarship.

635

636 **References**

637

- 638 [1] Y. Su, J. Li, C. Wu, P. Wu, Z.-X. Li, Influences of nano-particles on dynamic
639 strength of ultra-high performance concrete, *Composites Part B: Engineering* 91 (2016)
640 595-609.
- 641 [2] Y. Su, C. Wu, J. Li, Z.-X. Li, W. Li, Development of novel ultra-high performance
642 concrete: From material to structure, *Construction and Building Materials* 135 (2017)
643 517-528.
- 644 [3] Y.N. Chan, X. Luo, W. Sun, Compressive strength and pore structure of
645 high-performance concrete after exposure to high temperature up to 800°C, *Cement
646 and Concrete Research* 30 (2000) 247-251.
- 647 [4] G. Choe, G. Kim, N. Gucunski, S. Lee, Evaluation of the mechanical properties of
648 200MPa ultra-high-strength concrete at elevated temperatures and residual strength of
649 column, *Construction and Building Materials* 86 (2015) 159-168.
- 650 [5] Y.W. Lee, G.Y. Kim, N. Gucunski, G.C. Choe, M.H. Yoon, Thermal strain behavior
651 and strength degradation of ultra-high-strength-concrete, *Materials and Structures* 49(8)
652 (2015) 3411-3421.
- 653 [6] A.Q. Sobia, M.S. Hamidah, I. Azmi, S.F.A. Rafeeqi, Elevated temperature
654 resistance of ultra-high-performance fibre-reinforced cementitious composites,
655 *Magazine of Concrete Research* 67(17) (2015) 923-937.
- 656 [7] M. Xiong, J.Y. Richard Liew, Spalling behavior and residual resistance of fibre
657 reinforced Ultra-High performance concrete after exposure to high temperatures,
658 *Materiales de Construcción* 65(320) (2015) e071.
- 659 [8] M.-X. Xiong, J.Y.R. Liew, Mechanical behaviour of ultra-high strength concrete at
660 elevated temperatures and fire resistance of ultra-high strength concrete filled steel
661 tubes, *Materials & Design* 104 (2016) 414-427.
- 662 [9] C. Kahanji, F. Ali, A. Nadjai, Experimental study of ultra-high performance fibre
663 reinforced concrete under ISO 834 fire, *Structures in Fire (Proceedings of the Ninth
664 International Conference)*, 2016, pp. 165-173.
- 665 [10] C. Kahanji, F. Ali, A. Nadjai, Explosive spalling of ultra-high performance fibre
666 reinforced concrete beams under fire, *Journal of Structural Fire Engineering* 7(4) (2016)
667 328-348.
- 668 [11] W.M. Lin, T.D. Lin, L.J. Powers-Couche, Microstructures of fire-damaged
669 concrete, *ACI Materials Journal* 93(3) (1996) 199-205.
- 670 [12] A.H. Akca, N. Özyurt Zihnioğlu, High performance concrete under elevated
671 temperatures, *Construction and Building Materials* 44 (2013) 317-328.
- 672 [13] V. Ducman, A. Mladenović, The potential use of steel slag in refractory concrete,
673 *Materials Characterization* 62(7) (2011) 716-723.
- 674 [14] X. Guo, H. Shi, K. Wu, Effects of steel slag powder on workability and durability
675 of concrete, *Journal of Wuhan University of Technology-Mater. Sci. Ed.* 29(4) (2014)
676 733-739.
- 677 [15] I. Netinger, D. Bjegović, G. Vrhovac, Utilisation of steel slag as an aggregate in
678 concrete, *Materials and Structures* 44(9) (2011) 1565-1575.
- 679 [16] H. Qasrawi, F. Shalabi, I. Asi, Use of low CaO unprocessed steel slag in concrete
680 as fine aggregate, *Construction and Building Materials* 23(2) (2009) 1118-1125.
- 681 [17] İ. Yüksel, R. Siddique, Ö. Özkan, Influence of high temperature on the properties
682 of concretes made with industrial by-products as fine aggregate replacement,
683 *Construction and Building Materials* 25(2) (2011) 967-972.

684 [18] I. Netinger, D. Varevac, D. Bjegović, D. Morić, Effect of high temperature on
685 properties of steel slag aggregate concrete, *Fire Safety Journal* 59 (2013) 1-7.

686 [19] Y. Su, J. Li, C. Wu, P. Wu, Z.-X. Li, Effects of steel fibres on dynamic strength of
687 UHPC, *Construction and Building Materials* 114 (2016) 708-718.

688 [20] S. Pyo, H.-K. Kim, Fresh and hardened properties of ultra-high performance
689 concrete incorporating coal bottom ash and slag powder, *Construction and Building*
690 *Materials* 131 (2017) 459-466.

691 [21] P.S. Ambily, C. Umarani, K. Ravisankar, P.R. Prem, B.H. Bharatkumar, N.R. Iyer,
692 Studies on ultra high performance concrete incorporating copper slag as fine aggregate,
693 *Construction and Building Materials* 77 (2015) 233-240.

694 [22] Y. Biskri, D. Achoura, N. Chelghoum, M. Mouret, Mechanical and durability
695 characteristics of High Performance Concrete containing steel slag and crystalized slag
696 as aggregates, *Construction and Building Materials* 150 (2017) 167-178.

697 [23] K.S. Al-Jabri, A.H. Al-Saidy, R. Taha, Effect of copper slag as a fine aggregate on
698 the properties of cement mortars and concrete, *Construction and Building Materials*
699 25(2) (2011) 933-938.

700 [24] I. Netinger, M.J.R. & D. Bjegović, A. Mladenović, Concrete containing steel slag
701 aggregate: Performance after high temperature exposure, in: A.e.a. (eds) (Ed.) *Concrete*
702 *Repair, Rehabilitation and Retrofitting III*, Taylor & Francis Group, London, 2012.

703 [25] W. Zheng, H. Li, Y. Wang, Compressive behaviour of hybrid fiber-reinforced
704 reactive powder concrete after high temperature, *Materials & Design* 41 (2012)
705 403-409.

706 [26] B. Nagy, D. Szagri, Hygrothermal Properties of Steel Fiber Reinforced Concretes,
707 *Applied Mechanics and Materials* 824 (2016) 579-588.

708 [27] G.-F. Peng, W.-W. Yang, J. Zhao, Y.-F. Liu, S.-H. Bian, L.-H. Zhao, Explosive
709 spalling and residual mechanical properties of fiber-toughened high-performance
710 concrete subjected to high temperatures, *Cement and Concrete Research* 36(4) (2006)
711 723-727.

712 [28] I. Hager, Behaviour of cement concrete at high temperature, *Bulletin of the Polish*
713 *Academy of Sciences: Technical Sciences* 61(1) (2013) 145-154.

714 [29] G. Debicki, R. Haniche, F. Delhomme, An experimental method for assessing the
715 spalling sensitivity of concrete mixture submitted to high temperature, *Cement and*
716 *Concrete Composites* 34(8) (2012) 958-963.

717 [30] F. Aslani, B. Samali, High Strength Polypropylene Fibre Reinforcement Concrete
718 at High Temperature, *Fire Technology* 50(5) (2013) 1229-1247.

719 [31] D.C. Okpala, Pore structure of hardened cement paste and mortar, *The*
720 *International Journal of Cement Composites and Lightweight Concrete* 11(4) (1989)
721 245-254.

722 [32] C. Gallé, Effect of drying on cement-based materials pore structure as identified by
723 mercury intrusion porosimetry: A comparative study between oven-, vacuum-, and
724 freeze-drying, *Cement and Concrete Research* 31 (2001) 1467-1477.

725 [33] ISO 834-1-1999 (E), Fire-resistance tests - Elements of building construction -
726 Part 1: General requirements, International Organization for Standardization, Geneva,
727 1999.

728 [34] W. Khaliq, V. Kodur, Thermal and mechanical properties of fiber reinforced high
729 performance self-consolidating concrete at elevated temperatures, *Cement and*
730 *Concrete Research* 41(11) (2011) 1112-1122.

731 [35] ASTM Standard E831-14, Standard test method for linear thermal expansion of
732 solid materials by thermomechanical analysis, ASTM International, West
733 Conshohocken, PA, 2014.

734 [36] L. Chen, Q. Fang, X. Jiang, Z. Ruan, J. Hong, Combined effects of high
735 temperature and high strain rate on normal weight concrete, *International Journal of*
736 *Impact Engineering* 86 (2015) 40-56.

737 [37] Eurocode, European Committee for Standardization (CEN), EN 1992-1-2
738 Eurocode 2: Design of Concrete Structures, Brussels, 2004.

739 [38] Y. Tsuchiya, K. Sumi, Thermal decomposition products of polypropylene, *Journal*
740 *of Polymer Science: Part A-1* 7 (1969) 1599-1607.

741 [39] A.M. Rashad, Y. Bai, P.A.M. Basheer, N.C. Collier, N.B. Milestone, Chemical and
742 mechanical stability of sodium sulfate activated slag after exposure to elevated
743 temperature, *Cement and Concrete Research* 42(2) (2012) 333-343.

744 [40] Eurocode, European Committee for Standardization (CEN), EN 1993-1-2
745 Eurocode 3: Design of steel structures, Brussels, 2005.

746 [41] H. Li, Y. Wang, H. Xie, W. Zheng, Microstructure analysis of reactive powder
747 concrete after exposed to high temperature (in Chinese), *J. Huazhong Univ. of Sci. &*
748 *Tech. (Natural Science Edition)* 40(5) (2012) 71-75.

749 [42] G.A. Khoury, B.N. Grainger, P.J.E. Sullivan, Transient thermal strain of concrete:
750 literature review, conditions within specimen and behaviour of individual constituent,
751 *Magazine of Concrete Research* 37(132) (1985) 131-144.

752 [43] A. Mendes, J. Sanjayan, F. Collins, Phase transformations and mechanical strength
753 of OPC/Slag pastes submitted to high temperatures, *Materials and Structures* 41(2)
754 (2007) 345-350.

755 [44] B. Jia, *Static and Dynamic Mechanical Behavior of Concrete at Elevated*
756 *Temperature (in Chinese)*, College of Civil Engineering of Chongqing University, 2011,
757 p. 146.

758 [45] H.Y. Su, J.Y. Xu, W.B. Ren, Experimental study on the dynamic compressive
759 mechanical properties of concrete at elevated temperature, *Materials & Design* 56
760 (2014) 579-588.

761